AJR FOCUS ON:

The Challenge of Detector Designs for PET

Thomas K. Lewellen[1]

OBJECTIVE. The use of PET, especially the use of PET/CT scanners, has expanded rapidly over the past few years. Although most of the detector development efforts have been focused on scintillator-based designs, other technologies, such as wire chambers, time projection chambers, and solid-state devices, are also being pursued.

CONCLUSION. Many of these new technologies have not translated into commercial systems. This article will explore some of the basic challenges of PET detector designs.

An Overview

A key component of a PET system is the detection of the coincident gamma rays associated with positron decay. In the process of designing PET detectors for these tasks, many compromises must be made between the ultimate spatial resolution, sensitivity, factors affecting the final image signal-to-noise ratio, and the cost of production. This author and others have previously published review articles on PET detector and scanner technology [1–12]. The goal of the present article is to review some of the challenges in PET detector development, focusing on scintillator-based designs because they are the dominant technology used in most PET scanners. However, the basic challenges for such detectors are similar no matter what technology is used.

To that end, we will somewhat arbitrarily define several general target areas: preclinical (e.g., animal) imaging, dedicated limited area scanners (e.g., neuroimaging or breast imaging), and whole-body imaging. We can further subdivide each of these three target areas into two additional categories: academic development and commercial development. This latter distinction highlights the different goals between "one-off" systems often developed in academic laboratories compared with the continuing evolution of systems that is more common for commercial vendors. We will not try to review all the details of PET scanner operation (detection and image reconstruction) because that topic is well covered in the review articles referenced in the previous paragraph.

The key role of the detector is to interact with the incoming gamma ray, locate the event in the detector array, determine when the event occurred, and determine how much energy was deposited in the detector by the gamma ray. An ideal detector should have high stopping power (i.e., a high probability that a 511 keV gamma ray will be totally absorbed by the detector), have high spatial resolution (i.e., the ability to determine the interaction location of the gamma ray in the detector to a small spatial volume), have very good energy resolution (to reduce the acceptance of scattered and random events), have very high timing resolution, and be inexpensive to produce.

A system designer has to find the compromises between detector designs for the list of parameters in the previous paragraph in terms of the tasks the final scanner is expected to perform. For example, preclinical systems targeted for mouse scanning need to have very high spatial resolution and enough sensitivity to be able to use that resolution, but they do not generally need outstanding energy resolution or very fast timing. Current whole-body scanners can seldom use their existing spatial resolution limits and are instead limited by counting statistics. Instead, designers of such systems are looking at ways to increase sensitivity (e.g., smaller detector rings or longer axial fields of view) or much improved timing to allow the use of time-of-flight (TOF) image reconstruction algorithms to improve the image signal-to-noise ratio.

Scintillation Detectors and Some Detector Basics

First, we will discuss some of the challenges in spatial resolution. Figure 1 (pixilated detec-

Keywords: detectors, PET

DOI:10.2214/AJR.10.4741

Received April 5, 2010; accepted after revision May 20, 2010.

[1]Division of Nuclear Medicine, University of Washington Medical Center, 222 Old Fisheries Science Center, 1959 NE Pacific Ave., Seattle, WA 98195. Address correspondence to T. K. Lewellen (tkldog@u.washington.edu).

AJR 2010; 195:301–309

0361–803X/10/1952–301

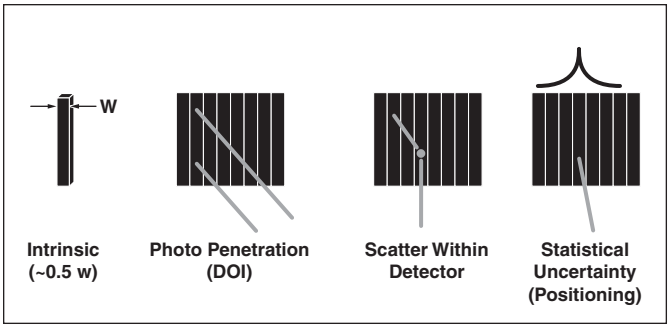

Fig. 1—Some factors that degrade spatial resolution in pixelated detector array. Photon penetration results in incorrect assignment of line of response in scanner if depth-of-interaction (DOI) is not able to be measured. Scatter within detector results in degraded crystal identification. Statistical uncertainty reflects errors in decoding process due to statistics of amount of light collected. w = crystal width.

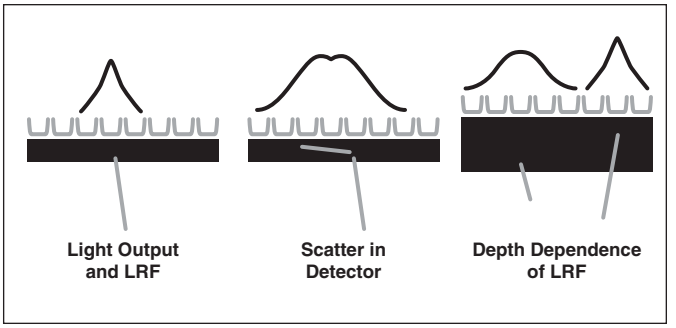

Fig. 2—Some factors that degrade spatial resolution in continuous crystal detector design. Light output and response function reflect both light sampling and statistics of amount of light collected. Scatter in detector and depth of interaction and the resulting change in light response function (LRF) generally lead to loss of spatial resolution due to changes in LRF.

tors) and Figure 2 (monolithic crystals) depict some of the major factors that affect detector performance. The intrinsic resolution of a pixilated detector is limited by the size of the crystal. However, just making crystals smaller does not necessarily scale the spatial resolution directly. Gamma rays not normally at the front entrance of an array of crystals can penetrate into the array, leading to an incorrect estimate of the line of response (LOR)—the line between two events detected in coincidence—if the detector system only identifies in which crystal the interaction took place. This problem is usually referred to as parallax. The position estimation is further complicated by scattering within the detector array. For scintillators typically used in PET, about 50% of the events detected will interact more than once in the detector array. Finally, at least for our discussion here, there is the statistical uncertainty of the decoded information because of the Poisson processes connected with the generation of the detector signal. Similar compounding events also occur for monolithic detectors, as illustrated in Figure 2.

In addition to these intrinsic spatial resolution issues, there are the issues of energy resolution and timing resolution. Timing resolution is important in three ways: reduction of random events by using a tighter timing window, the ability to use TOF image reconstruction algorithms if the timing is fast enough (e.g., < 600 ps for current TOF implementations), and reduction of system dead time (which allows higher event rates). TOF is an area of major interest currently, so a brief reminder of why it improves image quality is appropriate (more details are given elsewhere [7, 13, 14]). We have already mentioned that the data are normally thought of as LORs—lines connecting the two detectors in a coincident event. TOF allows one to localize, to some extent, where along an LOR an event occurred. The improved localization provides more information to the reconstruction algorithm, which, in turn, provides better spatial resolution versus noise compared with non-TOF reconstructions for the same number of detected events. The better the TOF resolution, the better the localization. All of these issues apply to any detector design, whether based on scintillators, solid-state detectors, or gas or liquid detectors.

There are many ways to decode the detector signals. If a pixelated array of scintillators is used, the most common approach is to use a coarse array of sensors to read out the light emitted from the crystal array (i.e., many crystals on one photosensor, often referred to as a block detector design). This approach reduces the number of photosensors and associated electronics, making for a more cost-effective solution at the expense of the ultimate intrinsic spatial resolution possible from the pixelated array, as described by Moses and Derenzo [15]. These detectors are typically read out using a modified Anger approach in most system designs [16–20]. There are also options to use monolithic crystals, and some commercial PET system designs used large plates of NaI(Tl) scintillators for readout [21, 22]. Although essentially all current commercial PET systems use pixelated designs, there has been a resurgence of the use of monolithic crystal de-

TABLE 1: Properties of Some Scintillators Used in PET Detectors

Property	NaI(Tl)	BaF_2	BGO	LSO	GSO	LYSO	$LaBr_3$	LFS	LuAP	LuI_3
Effective atomic no. (Z)	51	54	74	66	59	60	47	63	65	60
Linear attenuation coefficient (cm^{-1})	0.34	0.44	0.92	0.87	0.62	0.86	0.47	0.82	0.9	~0.56
Density (gm/cm^3)	3.67	4.89	7.13	7.4	6.7	7.1	5.3	7.3	8.34	5.6
Index of refraction	1.85	—	2.15	1.82	1.85	1.81	1.88	1.78	1.95	—
Light yield (% NaI(Tl))	100	5	15	75	30	80	160	77	16	190
Peak wavelength (nm)	410	220	480	420	430	420	370	430	365	470
Decay constant (ns)	230	0.8	300	40	65	41	25	35	18	30
Hydroscopic	Yes	Slight	No	No	No	No	No	No	No	Yes

Note—Some of these specifications are subject to change as developers change dopants and trace elements in the scintillator growth. For example, the light output, peak wavelength, decay time, and density for LYSO and LFS will vary somewhat for different versions of the basic scintillator. Dashes indicate a lack of consensus in the literature for the correct value. Nal (T1) = Thallium doped sodium iodide, BaF2 = barium floride, BGO = bismuth germinate, LSO = lutetium oxyorthosilicate, GSO = germanium orthosilicate, LYSO = lutetium ytrium orthosilicate, LaBr3 = lanthanum bromide, LFS = commercial variant of LSO (dopment proprietary), LuAP = lutetium orthoaluminate, LuI3 = lutetium iodide.

signs in the academic world, particularly for some preclinical scanner designs. With these designs, there has also been a move away from the traditional Anger logic style of decoding toward implementation of statistical estimation algorithms to locate an event in two or three dimensions [23–26].

The ideal scintillator (i.e., one that is fast, dense, with high light output, and inexpensive to produce) has yet to be found. Table 1 lists some of the parameters of many of the scintillators that have been investigated for use in PET. The main scintillators currently in use for PET detectors are BGO and variants of LSO (e.g., LSO, LYSO, and LFS). The LSO and its variants have grown in popularity because of its relatively high light output, good stopping power, and fast timing. Currently, all commercial TOF PET scanners use LSO and LYSO, as do most of the preclinical scanners currently on the market and in development in academic centers. Scintillation detectors with photomultiplier tubes (PMTs) have been the basic detector approach for most scanners. Given the long history of developers working with PMTs and scintillators, the technology is generally mature with proven electronics and fully developed supporting electronics and fabrication techniques.

What are the design directions that are being pursued for scintillation detectors? We will begin with whole-body imaging systems. For most applications, the modern commercial scanners are limited by sensitivity. One approach to increase sensitivity is to increase the solid angle of the detector array. For most scanners, that would mean increasing the axial field of view. Such a change would increase the cost of the scanner because of the increased volume of the scintillator and increased number of electronics channels needed. One partial solution would be to reduce the detector ring diameter, thus reducing the volume of scintillator, but that would increase the parallax error. The parallax error can be addressed by modeling the point spread function (the detector response) in the reconstruction algorithm, developing a depth-of-interaction detector system, or both. Thus, the challenge here is to develop a cost-effective method to implement a depth-of-interaction detector system.

Another approach, already implemented by the major PET system vendors, is to use TOF image reconstruction to improve the image quality. As timing improves, image quality improves significantly for TOF reconstructions (current commercial systems offer 500–700 ps resolution). What are the major possibilities to improve TOF resolution? Two of the areas of development are scintillators and photosensors. New scintillators that offer fast timing and high light output are certainly being investigated. At least one academic center has built a scanner with timing resolution on the order of 300 ps using $LaBr_3$ [13, 14].

Multimodality

To further complicate the challenges engineers must face is the emphasis on multimodality imaging systems. PET/CT began as an academic project, funded by the National Institutes of Health, with a commercial partner [27] and has become a commercial success with all the major vendors offering such systems. Although there is some effort in combined optical and PET scanners for preclinical applications [28–30], most academic and commercial efforts in exploration of new detectors are focused on the challenges of MR PET applications. One approach has been to use fiber optics to couple scintillation crystals to either PMTs, which are positioned at the far edge of the magnet fringe field [31, 32], or to solid-state photosensors, which are at the end of the magnet bore [33]. Using long fiberoptic bundles tends to lose light (degrade detector decoding), and the difficulties in coupling the fiber bundles to the scintillators and then routing out of the magnet also tend to limit the axial extent of the PET detector array.

As a result, others have investigated detectors using solid-state photosensors coupled directly to the crystals within the magnet bore. One of the challenges is the handling of the PET data, either having to route a great many signals out of the bore to the acquisition electronics or having to design a large portion of the electronics to work within the magnet bore to reduce the number of signals that have to be routed out of the magnet room. There are also developments for preclinical applications using special magnets with gaps to allow placing more conventional PET detector designs within the magnet system [34]. However, most solutions are based on detectors placed inside the magnet bore without modifications to the magnet itself. For example, both preclinical and human brain imaging inserts have been built for MRI systems using avalanche photodiodes (a type of solid-state light sensor) with the preamplifiers within the magnet bore and the remaining electronics outside of the magnet [35, 36]. Others have taken the majority of the electronics within the magnet bore, which greatly reduces the number of signals that must be routed out of the magnet room. There are many more innovative approaches being investigated on how to assemble, operate, and get the data out of PET inserts, but we will mention only one other example here, the Hyper Image project in the European Union, because it has an informative Web site (www.hybrid-pet-mr.eu) and has the ambitious goal of producing an MR TOF PET whole-body scanner. A key component of any of these systems is the PET detector, and because most designs use scintillators, we should take a closer look at photodetectors.

Photodetectors

PMTs are the most common photosensors in use. They have very high gain (typically approximately $\times 10^6$), low noise, fast response, and relatively low cost. The detector designer can now use PMTs with multiple dynode chains or channels (effectively multiple PMTs) inside a common vacuum envelope. Each channel provides an essentially independent photodetector. Work continues to improve PMTs, particularly in terms of timing response for TOF applications, and a designer has a large range of cost and performance parameters from which to choose.

There are also wide ranges of solid-state photosensors that have been considered for PET. These alternatives to PMTs address designs where one-on-one coupling is desired, layers of crystals and photosensors are used, there is a need for a general reduction in the volume of the photosensor, and applications such as PET detectors operate in a MRI system. More details are given in other review articles already referenced [6, 12], but the list includes silicon PIN diodes, avalanche photodiodes, and Geiger-mode avalanche photodiodes (often referred to as a silicon photomultiplier). Avalanche photodiodes have relatively good gain (~ 10^2–10^3 vs ~ 10^6 for PMTs) and can be fabricated as single-sensor devices, arrays, or as position-sensitive planar devices (position-sensitive avalanche photodiodes). The latter devices use signals from the four corners of the device to determine the position of an event much like the technique used in the original block detectors. Avalanche photodiodes have been used in several academic systems [33, 36–45], and at least one prototype human head PET insert for MRI scanners has been developed by a commercial vendor [35]. Figure 3

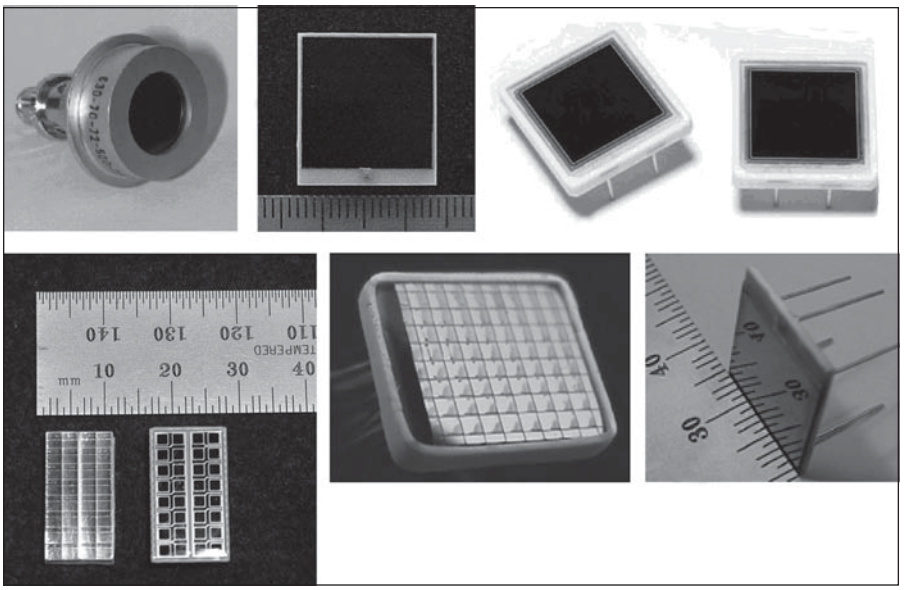

Fig. 3—Examples of avalanche photodiodes. Devices are available in a variety of packages in both single pixel and arrays as well as position-sensitive planar devices. Such devices have reasonable gains (~ 10^2) and can be used in magnetic fields.

depicts some of the many formats available of avalanche photodiodes.

The new photosensors getting the most attention as a possible alternative to PMTs are Geiger-mode avalanche photodiodes [9, 46–49]. The basic concept is built around avalanche photodiode microcells (Fig. 4). Each cell is an independent Geiger-mode detector such that a photon depositing energy in it causes it to discharge (i.e., produce a current). That discharge is then quenched, typically via a resistor connecting the microcell to the bias supply. There are many different designs of the microcells and surrounding substrates [9, 50] and we will not go into them here. These devices typically have gains of ~ 10^4–10^6 with bias voltages of 30–150 V, depending on the specific device. Time resolutions of 100 ps have been obtained for single photons, and investigators have reported coincident timing resolutions as low as 190 ps with scintillators. Thus, the devices have considerable potential for TOF PET applications, as well as for designs requiring compact or MRI-compatible detectors. As with other solid-state devices, Geiger-mode avalanche photodiodes work well in strong magnetic fields, such as in MRI scanners. There are some challenges in using the devices, such as dark current, temperature dependence of the gain, and getting elements in an array of Geiger-mode avalanche photodiodes devices to have the same bias requirements and gain response. Great progress has been made in lowering the cost of these devices, but it still takes a lot of silicon to cover the scintillator surfaces in a modern whole-body PET scanner, and the Geiger-mode avalanche photodiodes costs are not yet low enough to challenge the cost-effectiveness of PMTs. However, the potential for a relatively low-cost MRI-compatible high-gain photosensor remains, and Geiger-mode avalanche photodiodes are being incorporated in many scanner design studies.

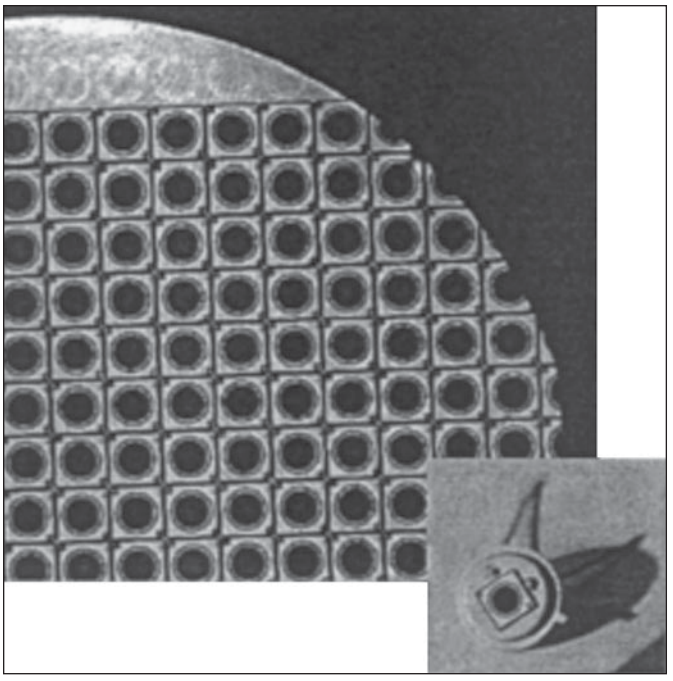

Fig. 4—Example of Geiger-mode avalanche photodiode. Series of avalanche photodiode microcells are connected via resistance in surrounding silicon. When photon interacts in cell, it discharges and then is quenched via resistance, coupling it to voltage supply. When coupled to scintillator, light photons that are emitted by scintillator cause many cells to fire, producing analog-like output signal simlar to that seen in photomultiplier tubes.

Depth of Interaction

Given that, in a typical detector, more than 50% of the events will include multiple interactions [51], an estimate of the depth of interaction to reduce parallax errors seems to be a worthy addition. Reduction of parallax errors can allow a designer to use a smaller detector ring diameter (reducing costs and improving sensitivity). Depth of interaction may also assist in the quest for better timing resolution. In long narrow crystals, the ultimate timing resolution is limited by the light path lengths in the crystal (most light photons will undergo many reflections in the crystal before escaping to be detected by a photosensor). The number of such reflections is somewhat dependent on where in the crystal the gamma ray interacts. Thus, a correction can be made for timing skewing depending on the point of interaction in the crystal, allowing improved timing resolution as developers push the current 500 ps timing being offered in commercial scanners.

For preclinical scanners, the parallax error is a major limitation of the final image's spatial resolution, and many designs have been developed to address the issue. If one wishes to estimate the point of first interaction, it generally requires that each interaction be individually identified (location and energy deposited) to work out the kinematics. If multiple interactions occur in one de-

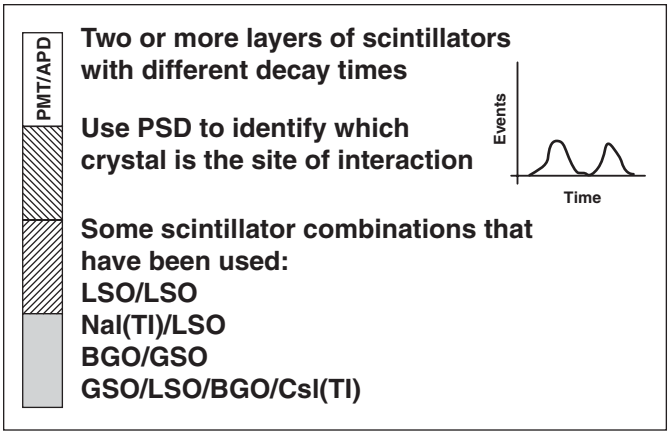

Fig. 5—Pulse shape discrimination (PSD)–based depth-of-interaction detector designs. Concept is to use two or more layers of crystals with different light decay times. Pulse shape analyzer can then be used to separate light from each layer based on its different decay times (and resulting pulse shape). BGO = bismuth germinate oxide, GSO = germanium silicate oxide, LSO = lutecium silicate oxide.

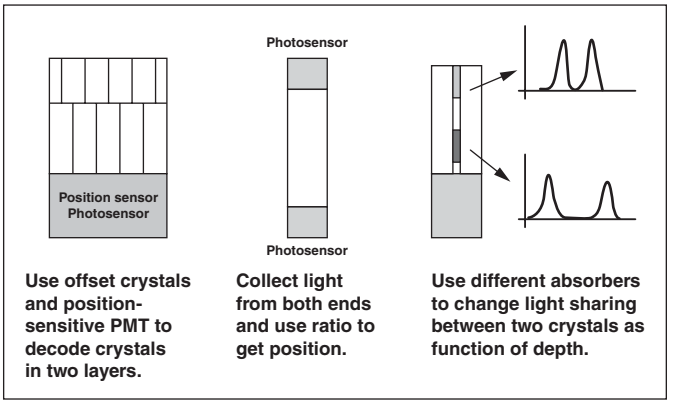

Fig. 6—Three approaches for depth-of-interaction detector modules. Layers of crystals are offset so that each crystal is visible in crystal map similar to that of Figure 5 (*left*). Light is collected from each end of crystal, and ratio of light collected provides depth-of-interaction information (*center*). Light is shared between paired crystals by modifying the common interface such that light at one end is not shared between photomultiplier tube (PMT) elements while light at the other end is shared ~ 50% (*right*). Ratio of light from the paired crystals provides depth-of-interaction information.

tector element, then the interactions are generally not separable, and thus only the depth of interaction of the centroid of the multiple interactions can be estimated. For pixelated detectors with detector elements on the order of 1 × 1 mm cross-sections, the vast majority of the multiple interactions will occur in separate elements. For example, with an LSO pixelated detector using 2 × 2 × 20 mm crystals, ~ 44% of the interactions will be single events with total absorption, and most of the events will have between two and five interactions in separate crystals in the array [51].

The main approaches to get the required information for point-of-first-interaction estimation generally use layers of small detector elements or methods to encode the depth of interaction in same manner. Many encoding approaches have been developed. One of the first is to use pulse shape discrimination, which exploits stacks of scintillator crystals with different decay times (Fig. 5). The differences in the resulting pulse shapes allow one to separate the crystal that is the source of the event [52–55]. To date, pulse shape discrimination has been used in preclinical and some dedicated brain scanners. Some of the limitations in the approach include cost of the fabrication of the detectors and the impact on timing resolution given the many different scintillators used.

Other examples of encoding approaches are depicted in Figure 6. One approach that has been used in many preclinical designs is that of offset layers of arrays of crystals. Investigators have progressed from two layers up to four layers [56, 57] and even eight layers by adding pulse shape discrimination [58]. One of the limitations is that, as more layers are added, there is more overlap between the decoded crystal positions (loss of intrinsic spatial resolution). Another is a loss of fast timing capability (for those applications that require TOF). Perhaps the most common depth-of-interaction approach has been the use of double-ended sensors to read the ratio of light collected at both ends of a crystal. There have been many implementations of this approach, dating back to the early 1990s [59]. Figure 7 depicts one such design using a pair of positron-sensitive avalanche photodiodes to achieve a depth of interaction of ~ 2 mm with illumination of the detector from the side with a collimated beam [60]. Similar results have been obtained with Geiger-mode avalanche photodiodes coupled to single crystals [61]. Work has also been done using double-sided readout of large monolithic crystals [62].

One complication of the double-ended approach is the fabrication challenges with sensors on both sides of the crystals (e.g., extra connectors, electronics channels, and mounting issues). There are also efforts to obtain depth-of-interaction decoding with single-ended readouts. One solution is to share light between pairs of crystals (Fig. 6) so that the amount of light shared is related to depth of interaction [51, 63]. A disadvantage of many of these depth-of-interaction designs is the need for arrays of crystals. Although that is precisely what is done with current commercial systems, the cost of making the arrays is significant, particularly for very high-resolution per-clinical systems where one must deal with tens of thousands of small crystals. The alternative is to use monolithic crystals.

Monolithic crystal designs have been pursued by many investigators (Fig. 8). By us-

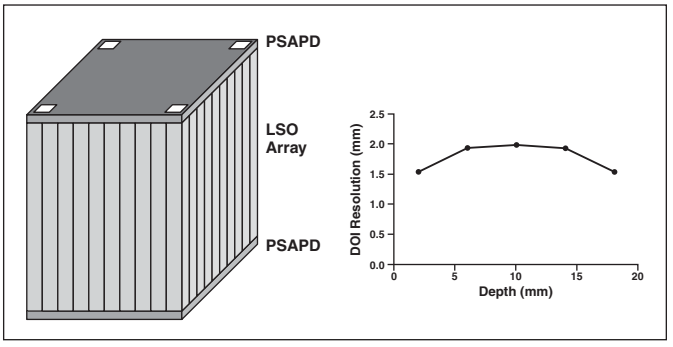

Fig. 7—Another depth-of-interaction (DOI) approach is to use positron-sensitive avalanche photodiode (PSAPD) at both ends of crystal array. DOI is determined by ratio of light detected at both ends of array. DOI data shown are from detector developed at University of California, Davis. LSO = lutecium silicate oxide.

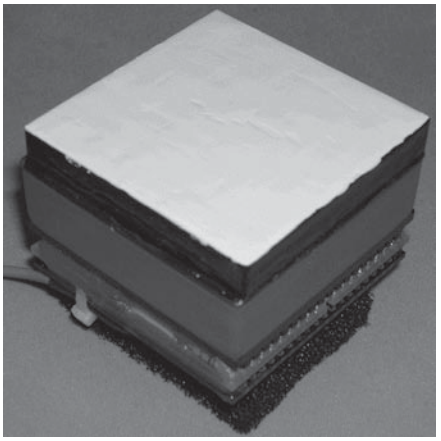

Fig. 8—Example of assembled thick slab detector. A 50 × 50 × 8 mm lutecium yttrium silicate oxide (LYSO) crystal is mounted to 64-anode photomultiplier tube.

ing statistical estimation techniques, designers have been able to use essentially all of the crystal area and still extract high intrinsic spatial resolution. Furthermore, by measuring the shape of the light response from the scintillator, the depth of interaction for the event can be estimated [64–66]. Because the measured shape is for all interactions of an event within the crystal, the point of first interaction cannot be estimated with any accuracy. However, the energy-weighted centroid of the multiple events can be estimated to an accuracy on the order of 2 mm, with an intrinsic spatial resolution of less than 1 mm [67]. The advantage of such designs is a reduction in cost by not using pixelated arrays. Furthermore, by using monolithic crystals with about the same overall cross-sectional area as a more conventional pixelated crystal array, the count rate capabilities of the two designs are equivalent. Thus, a large PET scanner could be built by tiling monolithic detectors in the same manner as crystal blocks are assembled today. The disadvantage is that the statistical estimation requires that all of the individual photosensor data be collected and processed and that the number of photosensors (sampling points) is adequate to measure the light response function. In short, a lot of data are collected for each event. With the advances in modern devices, such as field programmable gate arrays, it is possible to perform these estimates on the fly for each detector module [68]. In fact, the processing speeds are such that issues such as dead time comparing small monolithic (50 × 50 mm) to pixelated detectors using many-on-one decoding are not a major issue. Pixelated detectors using one-on-one decoding will have an advantage in count rate only if the supporting electronics are designed correctly. Thus, the choice in selecting one of these depth-of-interaction designs really comes down to a cost-benefit analysis that takes into account existing electronics designs that could be used to support whichever depth-of-interaction design is of interest and the desired maximum spatial resolution (in all three dimensions). At the moment, such detectors are more likely to be used in preclinical academic systems, where it is somewhat easier to justify the development (and cost) for the specialized electronics to implement the needed data processing.

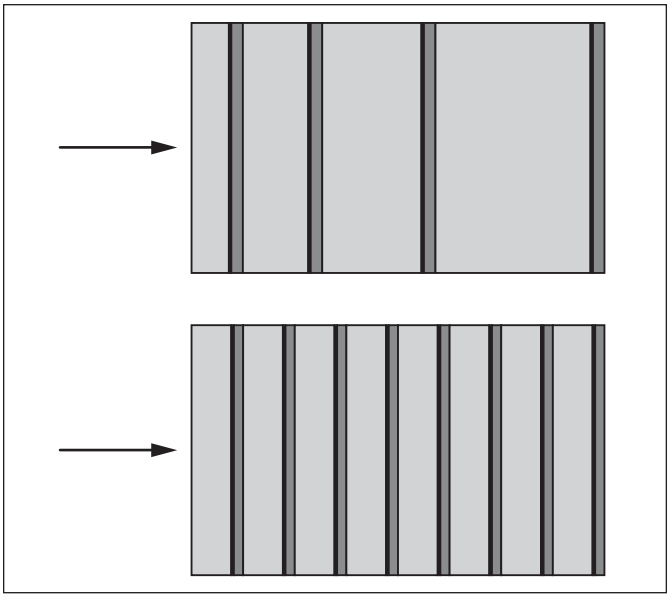

Fig. 9—Example of possible layered detector approach for depth-of-interaction determination with slabs of detectors layered along direction of incoming gamma rays. Both many thin layers (*bottom*) and layers with different thicknesses based on probability of interaction with depth (*top*) have been developed. By reading out each layer independently, measurements of location and energy deposited in each layered can be used to estimate point of first interaction within detector.

The layer approach (Fig. 9) simply stacks layers of thin detectors such that multiple interactions are likely to take place in separate layers. Each layer is then read out (position and energy deposited) for each event. In this way, high sensitivity can be maintained at the cost of a significant increase in the number of detector and electronics channels. One example of the layered approach with monolithic scintillation crystals is described by Moehrs et al. [69]. An example using matrixes of long scintillator readout with layers of fiber optics has been proposed by Braem et al. [70]. These approaches allow a designer to trade off depth-of-interaction and point-of-first-interaction capabilities, spatial resolution, and sensitivity by selecting the spatial (x, y, z) decoding schemes and the number of layers. An example of the impact of depth of interaction in a high-resolution application (in this case, breast imaging) is shown in Figure 10. In this figure, we show simulation data of a breast PET imager using the paired crystal light-sharing design shown in Figure 6 comparing a maximum likelihood reconstruction and a depth-of-interaction reconstruction using an estimate of the point of first interaction (Bayesian). As is the case with any scanner design, the more information we have of the interactions in the detectors, the better we can model the system in the image reconstruction algorithm. An alternative is to model the spatially variant point spread function (i.e., detector response) of the system for a non–depth-of-interaction detector and include the point spread function in the image reconstruction, as is being done in commercial PET scanners. The results are impressive, but they also lead to nonuniform noise correlations that some find objectionable, and the system modeling affects the required computing power needed. The best of all worlds is likely to be a combination of both a depth-of-interaction detector and a model of the point spread function (after the depth-of-interaction information has been included) in the image reconstruction. Although performance can be very impressive, the cost and complexity of these designs have limited their deployment in fully functional scanner systems. Essentially all of these design concepts can be implemented with nonscintillation detectors. However, because most systems use scintillators, we will not review them here and only note a few references other than the aforementioned review articles [71–87].

Summary

One additional challenge we have not mentioned is that a detector designer must also

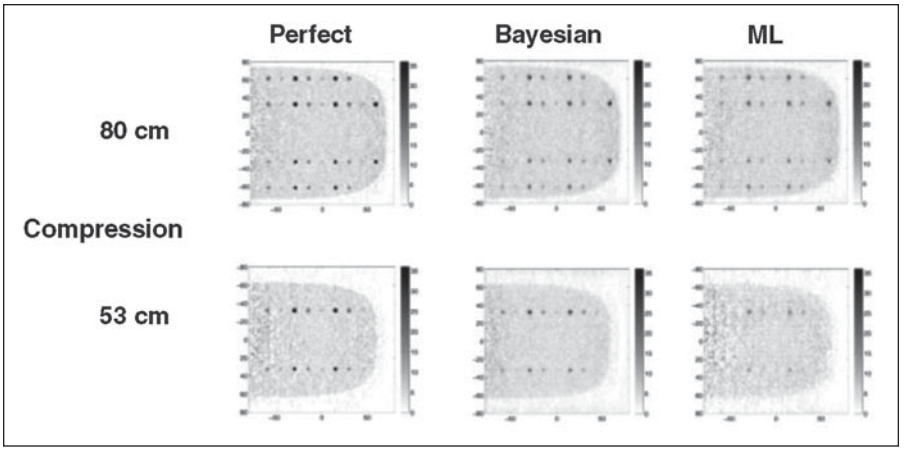

Fig. 10—Example of impact of depth-of-interaction in high-resolution application (in this case breast imaging). We show simulation data of breast PET imager using the paired crystal light-sharing design shown in Figure 6 comparing maximum likelihood (ML) reconstruction and depth-of-interaction reconstruction using estimate of point of first interaction (Bayesian).

consider the rest of the system architecture, especially the image reconstruction software. With the increase of computing power in typical scanners, image reconstruction algorithms have been able to include more accurate models of the various processes that affect image quality, such as the scanner nonstationary point response functions. Such algorithms can compensate for some of the multiple interaction issues in the detector performance. Thus, a detector designer does not necessarily have to focus on the ideal detector but rather on the ideal system. For example, the degree to which depth of interaction or point of first interaction needs to be measured to affect the final image quality will also be a function of how well the image reconstruction algorithms can compensate for nonideal detector response.

Whatever technology is used, the basic features of the yet to be realized ideal detector we mentioned earlier in this article remain the same. The capabilities of modern scanners have continued to improve, with preclinical systems starting to push the 500–700 μm resolution range in the academic laboratories and commercial whole-body scanners adding TOF and starting to push the TOF resolution below 500 ps. The optimization of any scanner is a complex task, of which the detector is just the starting point. The continued research and development in this area and the continued improvements we have seen hold considerable promise for the continued evolution of the PET scanner as a valuable tool in metabolic imaging.

Acknowledgments

I am indebted to all the members of the Nuclear Medicine Physics Group at the University of Washington for making it possible for me to find the time to write this article and for their insight and good work that has allowed our laboratory to work on detector and scanner development so consistently over the years. In particular, I thank Robert Miyaoka for his fine work on the MiCES detectors, Larry MacDonald, Wendy McDougald, and William Hunter for their work on our depth of interaction and MR detector projects as well as Robert Harrison for development of the simulation tools we use routinely in our work. I also am happy to acknowledge the patience and skills of Paul Kinahan and Adam Alessio in working with me on so many image reconstruction and data analysis tasks, in particular those dealing with modeling detector response in the image reconstruction algorithm. If space permitted, I would also list all of those investigators who have done so much for the field and have taken the time to assist my laboratory and me over the years. Last, but far from least, I thank the National Cancer Institute, the National Institute for Biomedical Imaging and Bioengineering, as well as GE Healthcare, Philips Healthcare, Siemens Healthcare, Zecotek Photonics, and Altera corporation for their generous support of our laboratory.

References

1. Cherry SR. In vivo molecular and genomic imaging: new challenges for imaging physics. *Phys Med Biol* 2004; 49:R13–R48
2. Petegnief Y, Aubineau-Laniece I, Kerrou K, Jourdain JR, Talbot JN. Advanced radionuclide detection techniques for in vitro and in vivo animal imaging. *Cell Mol Biol* 2001; 47:443–451
3. Humm JL, Rosenfeld A, Del Guerra A. From PET detectors to PET scanners. *Eur J Nucl Med Mol Imaging* 2003; 30:1574–1597
4. Townsend DW. Physical principles and technology of clinical PET imaging. *Ann Acad Med Singapore* 2004; 33:133–145
5. Ziegler SI. Positron emission tomography: principles, technology, and recent developments. *Nucl Phys A* 2005; 752:679–687
6. Del Guerra A, Belcari N. State-of-the-art of PET scanners for small animal and breast cancer imaging. *Nucl Instrum Methods Phys Res A* 2007; 580:910–914
7. Moses WW. Recent advances and future advances in time-of-flight PET. *Nucl Instrum Methods Phys Res A* 2007; 580:919–924
8. Eriksson L, Townsend D, Conti M, et al. Future instrumentation in positron emission tomography. *2006 IEEE Nuclear Science Symposium Conference Record*. Washington, DC: IEEE, 2007; 2542–2545
9. Renker D. New trends in photodetectors. *Nucl Instrum Methods Phys Res A* 2007; 571:1–6
10. Del Guerra A, Belcari N. From man to mouse to cell…and back again. *Nucl Instrum Methods Phys Res A* 2007; 572:246–249
11. Trebossen R. Recent innovations in the detection systems of positron emission tomography. *Medecine Nucleaire Med Nucl* 2007; 31:126–131
12. Lewellen TK. Recent developments in PET detector technology. *Phys Med Biol* 2008; 53:R287–R317
13. Glodo J, Kuhn A, Higgins WM, et al. CeBr3 for time-of-flight PET. *2006 IEEE Nuclear Science Symposium Conference Record*. Washington, DC: IEEE, 2007; 1570–1573
14. Kuhn A, Surti S, Karp JS, et al. Design of a lanthanum bromide detector for time-of-flight PET. *IEEE Trans Nucl Sci* 2004; 51:2550–2557
15. Moses WW, Derenzo SE. Empirical observation of resolution degradation in positron emission tomographs utilizing block detectors. *J Nucl Med* 1993; 34:101P
16. Cherry SR, Sorenson JA, Phelps ME. *Physics in nuclear medicine*. Orlando, FL: Saunders, 2003
17. Lewellen TK, Karp J. PET systems. In: Wernick MN, Aarsvold JN, eds. *Emission tomography: the fundamentals of PET and SPECT*. London, UK: Elsevier Academic Press, 2004: 179–194
18. St James S, Thompson CJ. Image blurring due to light-sharing in PET block detectors. *Med Phys* 2006; 33:405–410
19. Tomic N, Thompson CJ, Casey ME. Investigation of the "Block Effect" on spatial resolution in PET detectors. *IEEE Trans Nucl Sci* 2005; 52:599–605

20. Casey M, Nutt R. A multicrystal two dimensional BGO detector system for positron emission tomography. *IEEE Trans Nucl Sci* 1986; 33:460–463
21. Adam LE, Karp JS, Daube-Witherspoon ME, Smith RJ. Performance of a whole-body PET scanner using curve-plate NaI(Tl) detectors. *J Nucl Med* 2001; 42:1821–1830
22. Karp JS, Muehllehner G, Mankof F, et al. Continuous-slice PENN-PET: a positron tomograph with volume imaging capability. *J Nucl Med* 1990; 31:617–627
23. Ling T, Lewellen TK, Miyaoka RS. Depth of interaction decoding of a continuous crystal detector module. *Phys Med Biol* 2007; 52:2213–2228
24. Parra L, Barrett HH. List-mode likelihood: EM algorithm and image quality estimation demonstrated on 2-D PET. *IEEE Trans Med Imaging* 1998; 17:228–235
25. Joung J, Miyaoka RS, Lewellen TK. cMiCE: a high resolution animal PET using continuous LSO with a statistics based positioning scheme. *Nucl Instrum Methods* 2002; A489:584–598
26. Joung J, Miyaoka RS, Kohlmyer SG, Lewellen TK. Implementation of ML based positioning algorithms for scintillation cameras. *IEEE Trans Nucl Sci* 2000; 47:1104–1111
27. Townsend DW, Beyer T, Kinahan PE, et al. The SMART scanner: a combined PET/CT tomograph for clinical oncology. *IEEE Nuclear Science Symposium*. Washington, DC: IEEE, 1998; 2:1170–1174
28. Peter J, Schulz RB, Semmler W. PET-MOT: a novel concept for simultaneous positron and optical tomography in small animals. *IEEE Nuclear Science Symposium*. Washington, DC: IEEE, 2006; 1757–1760
29. Vu NT, Silverman RW, Chatziioannou AF. Preliminary performance of optical PET (OPET) detectors for the detection of visible light photons. *Nucl Instrum Methods Phys Res A* 2006; 569:563–566
30. Berard P, Riendeau J, Pepin CM, et al. Investigation of the LabPET™ detector and electronics for photon-counting CT imaging. *Nucl Instrum Methods Phys Res A* 2007; 571:114–117
31. Raylman RR, Majewski S, Lemieux SK, et al. Simultaneous MRI and PET imaging of a rat brain. *Phys Med Biol* 2006; 51:6371–6379
32. Mackewn J, Strul D, Hallett WA, et al. Design and development of an MR-compatible PET scanner for imaging small animals. *IEEE Nuclear Science Symposium Conference Record*. Washington, DC: IEEE, 2004; 5:3271–3274
33. Catana C, Wu Y, Judenhofer MS, Qi J, Pichler BJ, Cherry SR. Simultaneous acquisition of multislice PET and MR images: initial results with a MR-compatible PET scanner. *J Nucl Med* 2006; 47: 1968–1976
34. Lucas AJ, Hawkes RC, Ansorge RE, et al. Development of a combined microPET-MR system. *Technol Cancer Res Treat* 2006; 5:337–341
35. Schlemmer HP, Pichler BJ, Schmand M, et al. Simultaneous MR/PET imaging of the human brain: feasibility study. *Radiology* 2008; 248: 1028–1035
36. Grazioso R, Nan Z, Corbeil J, et al. APD-based PET detector for simultaneous PET/MR imaging. *Nucl Instrum Methods Phys Res A* 2006; 569:301–305
37. Judenhofer MS, Catana C, Swann BK, et al. PET/MR images acquired with a compact MR-compatible PET detector in a 7-T magnet. *Radiology* 2007; 244:807–814
38. Powolny F, Moraes D, Auffray E, et al. Development of a new photo-detector readout technique for PET and CT imaging. *Nucl Instrum Methods Phys Res A* 2007; 571:329–332
39. Bruyndonckx P, Lemaitre C, Schaart D, et al. Towards a continuous crystal APD-based PET detector design. *Nucl Instrum Methods Phys Res A* 2007; 571:182–186
40. Pichler BJ, Judenhofer MS, Catana C, et al. Performance test of an LSO-APD detector in a 7-T MRI scanner for simultaneous PET/MRI. *J Nucl Med* 2006; 47:639–647
41. McCallum S, Clowes P, Welch A. A four-layer attenuation compensated PET detector based on APD arrays without discrete crystal elements. *Phys Med Biol* 2005; 50:4187–4207
42. Burr KC, Ivan A, Astleberry DE, LeBlanc JW, Shah KS, Farrell R. Evaluation of a prototype small-animal PET detector with depth-of-interaction encoding. *IEEE Trans Nucl Sci* 2004; 51:1791–1798
43. McCallum S, Clowes P, Welch A. A multi layer detector for PET based on APD arrays and continuous crystal elements. *IEEE Nuclear Science Symposium Conference Record*. Washington, DC: IEEE, 2004; 5:2898–2902
44. Ziegler SI, Pichler BJ, Boening G, et al. A prototype high-resolution animal positron tomograph with avalanche photodiode arrays and LSO crystals. *Eur J Nucl Med* 2001; 28:136–143
45. Woody C, Schlyer D, Vaska P, et al. Preliminary studies of a simultaneous PET/MRI scanner based on the RatCAP small animal tomography. *Nucl Instrum Methods Phys Res A* 2007; 571:102–105
46. Herbert DJ, Moehrs S, D'Ascenzo N, et al. The silicon photomultiplier for application to high-resolution positron emission tomography. *Nucl Instrum Methods Phys Res A* 2007; 573:84–87
47. Musienko Y, Auffray E, Lecoq P, Reucroft S, Swain J, Trummer J. Study of multi-pixel Geiger-mode avalanche photodiodes as a read-out for PET. *Nucl Instrum Methods Phys Res A* 2007; 571:362–365
48. McElroy DP, Saveliev V, Reznik A, Rowlands LA. Evaluation of silicon photomultipliers: a promising new detector for MR compatible PET. *Nucl Instrum Methods Phys Res A* 2007; 571:106–109
49. Britvitch I, Johnson I, Renker D, Stoykov A, Lorenz E. Characterisation of Geiger-mode avalanche photodiodes for medical imaging applications. *Nucl Instrum Methods Phys Res A* 2007; 571:308–311
50. Renker D, Lorenz E. Advances in solid state photon detectors. *J Inst* 2009; 4:P04004
51. Champley KM, Lewellen TK, MacDonald LR, Miyaoka RS, Kinahan PE. Statistical LOR estimation for high-resolution dMiCE PET detector. *Phys Med Biol* 2009; 54:6369–6382
52. Costa E, Massaro E, Piro L. A BGO-CsI(TI) phoswich: a new detector for x-and y-ray astronomy. *Nucl Instrum Methods Phys Res A* 1986; A243: 572–577
53. Jin HJ, Yong C, Yong HC, et al. Optimization of optical coupling conditions for LSO/LuYAP phoswich detector. *2004 IEEE Nuclear Science Symposium Conference Record*. Washington, DC: IEEE, 2004; 5:2970–2974
54. Seidel J, Vaquero JJ, Gandler WR, Green MV. Depth identification accuracy of a three layer phoswich PET detector module. *IEEE Trans Nucl Sci* 1999; 46:485–490
55. Yong C, Jin Ho J, Yong Hyun C, et al. Optimization of LSO/LuYAP phoswich detector for small animal PET. *Nucl Instrum Methods Phys Res A* 2007; 571:669–675
56. Hasegawa T, Yoshida E, Kobayashi A, et al. Evaluation of static physics performance of the jPET-D4 by Monte Carlo simulations. *Phys Med Biol* 2007; 52:213–230
57. Nishikido F, Tsuda T, Inadama N, et al. Spatial resolution measured by a prototype system of two four-layer DOI detectors for jPET-RD. *IEEE Nuclear Science Symposium Conference Record*. Washington, DC: IEEE, 2007; 3041–3044
58. Inadama N, Murayama H, Tsuda T, et al. Optimization of crystal arrangement on 8-layer DOI PET detector. *IEEE Nuclear Science Symposium Conference Record*. Washington, DC: IEEE, 2007; 3082–3085
59. Moses WW, Derenzo SE, Nutt R, Digby WM, Williams CW, Andreaco M. Performance of a PET detector module utilizing an array of silicon photodiodes to identify the crystal of interaction. *IEEE Trans Nucl Sci* 1993; 40:1036–1040
60. Yang Y, Dokhale PA, Silverman RW, et al. Depth of interaction resolution measurements for a high resolution PET detector using position sensitive avalanche photodiodes. *Phys Med Biol* 2006; 51: 2131–2142
61. Shao Y, Li H, Gao K. Initial experimental studies of using solid-state photomultiplier for PET appli-

cations. *Nucl Instrum Methods Phys Res A* 2007; 580:944–950

62. Maas MC, Schaart DR, van der Laan DJ, et al. Monolithic scintillator PET detectors with intrinsic depth-of-interaction correction. *Phys Med Biol* 2009; 54:1893–1908
63. Lewellen TK, Janes M, Miyaoka RS. DMice: a depth-of-interaction detector design for PET scanners. *IEEE Nuclear Science Symposium and Medical Imaging Conference*. Washington, DC: IEEE, 2004; 2388–2392
64. Hunter WCJ, Barrett HH, Furenlid LR, Moore SK. Method of calibrating response statistics for ML estimation of 3D interaction position in a thick-detector gamma camera. *IEEE Nuclear Science Symposium Conference Record*. Washington, DC: IEEE, 2007; 4359–4363
65. Ling T, Burnett TH, Lewellen TK, Miyaoka RS. Parametric positioning of a continuous crystal PET detector with depth of interaction decoding. *Phys Med Biol* 2008; 53:1843–1863
66. Moore SK, Hunter WCJ, Furenlid LR, Barrett HH. Maximum-likelihood estimation of 3D event position in monolithic scintillation crystals: experimental results. *IEEE Nuclear Science Symposium Conference Record*. Washington, DC: IEEE, 2007; 3691–3694
67. Miyaoka RS, Li X, Lockhart C, Lewellen TK. Design of a high resolution, monolithic crystal, PET/MRI detector with DOI positioning capability. *IEEE Nuclear Science Symposium and Medical Imaging Conference Record*. Washington, DC: IEEE, 2008; 4688–4692
68. DeWitt D, Miyaoka RS, Xiaoli L, Lockhart C, Lewellen TK, Hauck S. Design of an FPGA based algorithm for real-time solutions of statistics-based positioning. *IEEE Nuclear Science Symposium and Medical Imaging Conference Record*. Washington, DC: IEEE, 2008; 5029–5035
69. Moehrs S, Del Guerra A, Herbert DJ, Mandelkern MA. A detector head design for small-animal PET with silicon photomultipliers (SiPM). *Phys Med Biol* 2006; 51:1113–1127
70. Braem A, Chesi E, Joram C, et al. Wavelength shifter strips and G-APD arrays for the read-out of the z-coordinate in axial PET modules. *Nucl Instrum Methods Phys Res A* 2008; 586:300–308
71. Ott RJ. Wire chambers revisited. *Eur J Nucl Med* 1993; 20:348–358
72. Schafers KP, Reader AJ, Kriens M, Knoess C, Schober O, Schafers M. Performance evaluation of the 32-module quadHIDAC small-animal PET scanner. *J Nucl Med* 2005; 46:996–1004
73. Tsyganov EN, Anderson J, Arbique G, et al. UTSW small animal positron emission imager. *IEEE Trans Nucl Sci* 2006; 53:2591–2600
74. Chepel VY. A new liquid xenon scintillation detector for positron emission tomography. *Nucl Tracks Radiat Meas* 1993; 21:47–51
75. Gallin-Martel ML, Martin P, Mayet F, et al. Experimental study of a liquid xenon PET prototype module. *Nucl Instrum Methods Phys Res A* 2006; 563:225–228
76. Doke T, Kikuchi J, Nishikido F. Time-of-flight positron emission tomography using liquid xenon scintillation. *Nucl Instrum Methods Phys Res A* 2006; 569:863–871
77. Amaudruz P, Bryman D, Kurchaninov L, et al. Investigation of liquid xenon detectors for PET: simultaneous reconstruction of light and charge signals from 511 keV photons. *IEEE Nuclear Science Symposium Conference Record*. Washington, DC: IEEE, 2007; 2889–2891
78. Gallin-Martel M-L, Gallin-Martel L, Grondin Y, et al. A liquid xenon positron emission tomograph for small animal imaging: first experimental results of a prototype cell. *Nucl Instrum Methods Phys Res A* 2009; 599:275–283
79. Amaudruz P, Bryman D, Kurchaninov L, et al. Simultaneous reconstruction of scintillation light and ionization charge produced by 511 keV photons in liquid xenon: potential application to PET. *Nucl Instrum Methods Phys Res A* 2009; 607:668–676
80. Cesca N, Auricchio N, Di Domenico G, et al. SiliPET: design of an ultra-high resolution small animal PET scanner based on stacks of semi-conductor detectors. *Nucl Instrum Methods Phys Res A* 2007; 572:225–227
81. Drezet A, Monnet O, Mathay F, Montemont G, Verger L. CdZnTe detectors for small field of view positron emission tomographic imaging. *Nucl Instrum Methods Phys Res A* 2007; 571:465–470
82. Vaska P, Bolotnikov A, Carini G, et al. Studies of CZT for PET applications. *IEEE Nuclear Science Symposium Conference Record*. Washington, DC: IEEE, 2006; 2799–2802
83. Levin CS, Foudray AM, Habte F. Impact of high energy resolution detectors on the performance of a PET system dedicated to breast cancer imaging. *Phys Med* 2006; 21[suppl 1]:28–34
84. Hadong K, Cirignano L, Dokhale P, et al. CdTe orthogonal strip detector for small animal PET. *IEEE Nuclear Science Symposium Conference Record*. Washington, DC: IEEE, 2007; 3827–3830
85. Chinn G, Foudray AMK, Levin CS. A method to include single photon events in image reconstruction for a 1 mm resolution PET system built with advanced 3-D positioning detectors. *IEEE Nuclear Science Symposium Conference Record*. Washington, DC: IEEE, 2007; 1740–1745
86. Cooper RJ, Turk G, Boston AJ, et al. Position sensitivity of the first SmartPET HPGe detector. *Nucl Instrum Methods Phys Res A* 2007; 573:72–75
87. Cooper RJ, Boston AJ, Boston HC, et al. SmartPET: applying HPGe and pulse shape analysis to small-animal PET. *Nucl Instrum Methods Phys Res A* 2007; 579:313–317